Functional MRI of Brain Activation Induced by Scanner Acoustic Noise

Peter A. Bandettini, A. Jesmanowicz, Joel Van Kylen, Rasmus M. Birn, James S. Hyde

A method is introduced by which brain activation caused by the acoustic noise associated with echo planar imaging (EPI) is mapped. Two types of time series were compared. The first time series, considered the "task," involved applying only EPI gradients for 20 s *without the application of RF pulses*, then, without pause, starting image collection. The second, considered the "control," involved typical sequential image acquisition without the prior gradient pulses. Subtraction of the first 5 s of the two time series revealed signal enhancement mainly in the primary auditory cortex. The technique was validated using a motor cortex task that mimicked the hypothesized scanner noise induced activation.

Key words: auditory cortex; BOLD contrast; acoustic noise; fMRI.

INTRODUCTION

A concern in functional magnetic resonance imaging (fMRI) studies (1–4) is that brain activation produced by MRI gradient switching acoustic noise may corrupt results primarily in studies of auditory cortex activation and of cognitive processes that may be modulated by ambient noise. Regions that have an elevated baseline level of activation may not be able to be as fully modulated between "resting" and "active" states. The reason for this may include saturation in the neuronal firing rate or in the hemodynamic response. These regions therefore might not appear as fully "activated" as with more silent functional imaging techniques. A few possible examples of this fMRI confound may include the relatively weak white noise activation (5), and mixed tonotopy results (6–8). This study begins to address this issue by introducing a method that allows the mapping of regions activated by the ambient scanner acoustic noise.

To map brain activation related to a stimulus, it is necessary to modulate the stimulus such that images collected during and between stimulus periods can be compared to create a functional image. The primary challenge in mapping regions activated by acoustic noise produced by gradient switching is that it is difficult to modulate the MRI related noise in a single time series or across time series without significantly changing imaging contrast parameters associated with the noise (i.e., TR, number of slices).

The strategy presented in this paper takes into consideration two factors: 1) The time for the longitudinal magnetization to reach steady state with successive RF excitations, and 2) the time for the activation-induced hemodynamic response to increase and reach a steady "on" state. Since activation-induced changes are highly localized and only on the order of 1%, it is important that longitudinal magnetization weighting is matched between images obtained during resting and active states. The time to reach steady state longitudinal magnetization depends on the flip angle, TR, and T_1 of the tissue. Typically, it is in the range of 4 to 6 s when imaging the brain, using a TR of 0.5 to 1 s, and using a flip angle of 60° to 85°. The time for the hemodynamic response to plateau in the "on" state is about 5 to 9 s (1–4, 9–11).

If the time to reach steady state magnetization were significantly less than the hemodynamic change time constant, then imaging activation by the scanner acoustic noise would be a simple process of subtracting the first several images in the time series, obtained before the hemodynamic response has a chance to plateau in the on state, from the later images in the time series. Because the time for longitudinal magnetization to reach steady state is similar to the hemodynamic response time, this type of subtraction would be dominated by differences in longi-

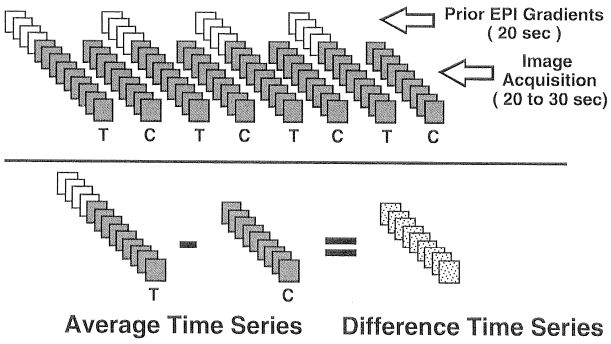

FIG. 1. Schematic illustration of the method by which regions activated by the acoustic noise of the scanner were mapped. For the "task" time series, labeled "T," *only the EPI gradient pulses* were applied for 20 s. Then, without pause, RF power and image acquisition was carried out for 30 to 40 s. These prior gradient pulses, indicated as white boxes, were applied for 20 s to allow for the EPI gradient acoustic noise induced hemodynamic response to reach a steady-state "on" state. For the "control" time series, labeled "C," image collection was performed without the prior 20 s of gradient pulses. At each time point, the "control" time series was subtracted from the "task" time series to create a "difference" series. During the first 4 to 8 s, which is the time that it takes for the hemodynamic response to increase and plateau, the two series differed in signal intensity in those regions activated by EPI gradient noise.

MRM 39:410–416 (1998)

From the Biophysics Research Institute, Medical College of Wisconsin, Milwaukee, Wisconsin.

Address correspondence to: Peter A. Bandettini, Ph.D., Biophysics Research Institute, Medical College of Wisconsin, 8701 W. Watertown Plank Road, Milwaukee, WI 53226.

Received February 11, 1997; revised July 11, 1997; accepted August 27, 1997.

This work was supported in part by grant MH51358 from the National Institutes of Health.

0740-3194/98 $3.00

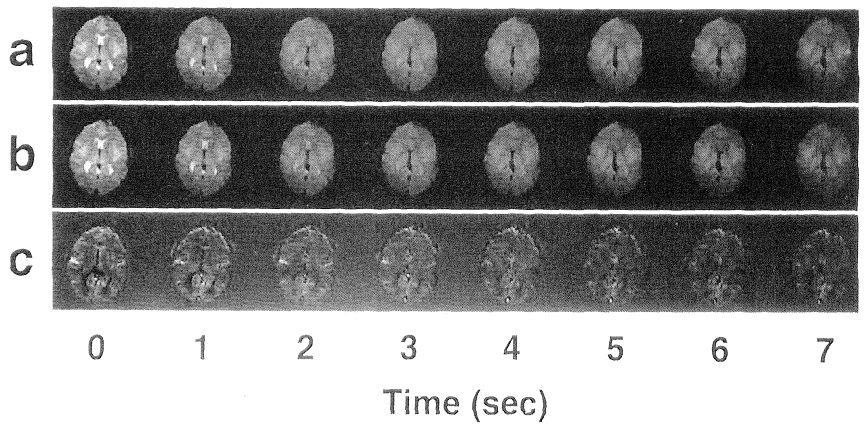

FIG. 2. The first seven images in the (a) "task" time series, and (b) "control" time series. (Matrix size = 64 × 64, FOV = 24 cm, TE = 40 ms, TR = 1000 ms, Thickness = 10 mm, θ = 85°). These images are the averaged from four interleaved "task" and "control" trials. (c) Time series of difference images produced by subtraction of each "control" from each "task" image. Signal enhancement is demonstrated bilaterally in the auditory cortex for the first 5 s, during which the BOLD signal in the "control" series is in the process of increasing as a result of the EPI gradient noise while the BOLD signal in the "task" series is already saturated in the "on" state.

tudinal magnetization (typically about 20% to 60%) and not by functionally related changes. This fact necessitated that two separate time series ("task" and "control") were collected so that longitudinal magnetization weighting at corresponding time points was identical.

In this study, image subtraction across two separate time series at each time point was performed, therefore matching longitudinal magnetization weighting in all images at all times. The first time series, considered the "control," involved typical acquisition of sequential blood oxygenation level dependent (BOLD) contrast-weighted images (1–4, 12). The second time series, considered the "task," involved first the application of *only* the EPI gradients in an identical manner as during image acquisition for about 20 s, and then without pause, starting RF excitation and image collection in the same fashion as in the control time series. The MRI signal during its approach to steady state longitudinal magnetization (first 5 to 7 s of acquisition) was identical between the two time series *except* in regions that had enhanced BOLD contrast (and possibly inflow contrast) due to neuronal activation-related hemodynamic changes induced by the noise of the prior gradient pulses. This localized signal intensity difference only existed during the time that the activation-induced hemodynamic response was in the process of reaching a steady-state "on" condition (about 5 to 7 s).

Two different studies incorporating this technique, each at a different TR value, were performed. The technique was further validated with the use of a well characterized motor cortex activation paradigm conducted to mimic auditory activation with and without prior gradient pulses.

METHODS

All studies were performed on a Bruker Biospec 3T/60 system. A balanced torque three axis gradient coil (13) and an endcapped birdcage transmit-receive RF coil (14) were used for EPI. In-plane voxel dimensions = 3.8 × 3.8 mm. Slice thickness = 10 mm. FOV = 24 cm. Matrix size = 64 × 64. For all studies, TE = 40 ms, TR = 0.5 s to 1 s, θ = 60° to 85°. The TR was chosen such that the transient hemodynamic onset curve would be adequately sampled. In-plane motion correction was performed on the averaged data set. Four male subjects, aged 24–30, were scanned. All subjects were instructed to remain motionless with eyes closed.

The basic technique is schematically shown in Fig. 1. Two types of time series were alternately acquired. The "task" time series, labeled "T," involved prior application of only EPI gradients in a similar manner as would be applied during image collection. No RF power was applied and therefore the magnetization in the imaging planes was not affected. These gradient pulses, indicated by the white boxes, were applied for 20 s to allow the hemodynamic response induced by the acoustic noise of the gradient pulses to reach a steady-state "on" condition. Immediately following this 20-s period, time-series image collection, indicated by the gray boxes, was started. Sequential images were then collected for about 30 to 40 s. During the first several seconds of the "task" series, longitudinal magnetization approached steady state, while the EPI acoustic noise induced activation was already plateaued in the "on" state.

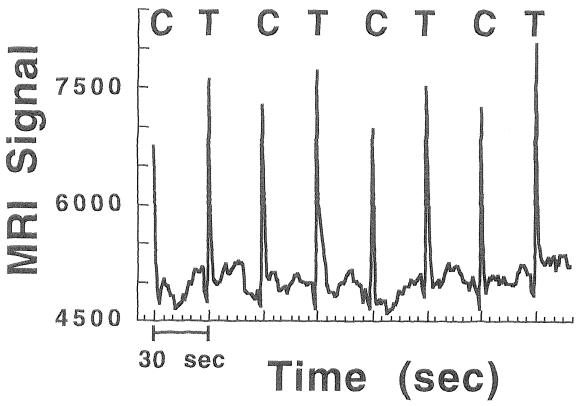

FIG. 3. MRI signal from 12 voxels in the auditory cortex during each of the four interleaved "control" (labeled "C") and "task" (labeled "T") trials. The highest signal intensity was at TR = ∞ at the start of each trial. The time to reach steady state longitudinal magnetization was about 5 seconds. Each successive trial was separated by about 1 min to allow the hemodynamic response to reach baseline.

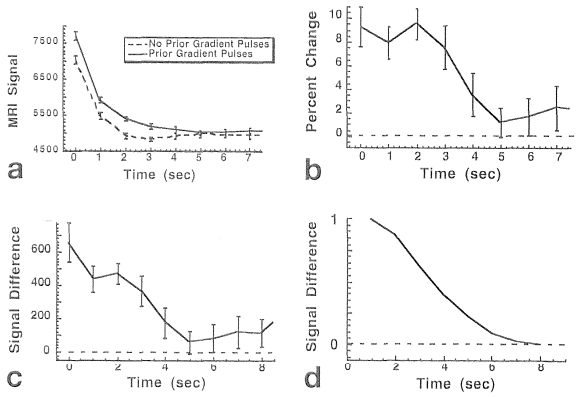

FIG. 4. (a) Average MRI signal from the four "control" and "task" trials in Fig. 3. (b) Average fractional difference signal between the "control" and "task" series. The difference returned to zero at about 5 s. (c) Average raw difference signal between the "control" and "task" series. This signal was used as the reference function for correlation analysis in the creation of the functional images in Fig. 5b. (d) Synthesized raw difference signal based on the expected hemodynamic response. This function was used as the reference function for correlation analysis in the creation of the functional images in Figure 5c.

The "control" time series, labeled "C," involved time-series collection of echo-planar images without the prior 20 s of gradient pulses. The "control" time series image collection was identical to the "task" time series collection. During the first several seconds of the "control" time series, magnetization was approaching steady state,

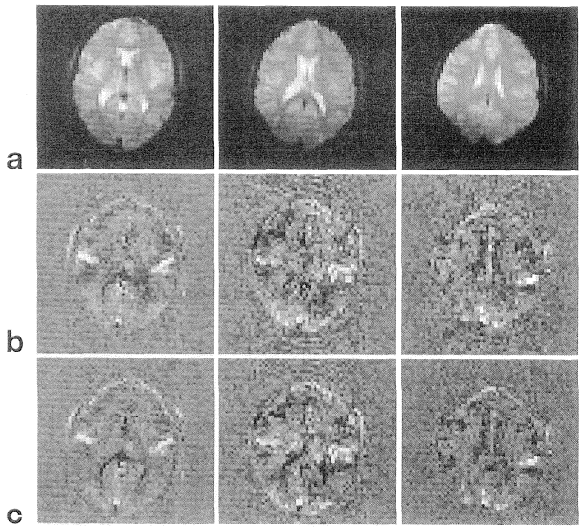

FIG. 5. (a) Anatomical images of the three slices obtained. In all images shown, the left side of the image corresponds to the subject's right hemisphere. The top is anterior. (b) Functional images corresponding to the anatomical images. These were created by calculation of the correlation coefficient of the difference signal, shown in Fig. 4c, with the difference image series. (c) Functional images created by calculation of the correlation coefficient of the synthesized difference signal, shown in Fig. 4d with the difference image series. Essentially, these images are a weighted average of the first seven difference images.

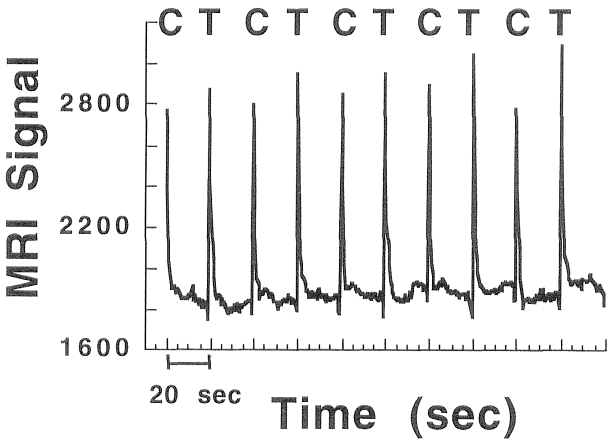

FIG. 6. MRI signal from 14 voxels in auditory cortex during each of the four interleaved "control" and "task" series. Here, the TR was 500 ms rather than 1000 ms.

and the EPI acoustic noise induced activation was just starting to increase.

As indicated in Fig. 1, the two types of time series were collected in an alternating manner and separated in time by about one minute to allow the hemodynamic response to reach baseline between the series. Three to five trials of each series were collected and averaged to produce an average "task" and "control" time series. Each "control" image was then subtracted from a "task" image at each corresponding point in time to create a "difference" time series.

Scanner noise activation was identified in two ways. The first method was by simple inspection of the sequential difference images during the first several seconds of image acquisition. The second method involved correlation analysis (15). A reference function was chosen from an ROI in auditory cortex. Correlation maps were created by voxel-wise calculation of the correlation coefficient of the unsmoothed reference function with the first 8 images in the "difference" time series. Correlation analysis using a reference function chosen from the data is potentially circular and misleading in that the reference function may have in it artifact that is not specific to activation. For comparison, a functional image for the data set in Study 1 was created using a synthesized reference function based on the expected hemodynamic response.

Three studies are presented. The first two demonstrate the technique. For these studies, the results from one subject demonstrating the clearest activation are shown. In this preliminary work, no further comparisons were made across subjects. The third study is a comparison, using motor cortex activation, of a functional image created using the above-described method with a functional image using the more conventional cyclic on-off paradigm.

In Study 1, three contiguous axial imaging planes containing auditory cortex were collected. TR = 1 s. $\theta = 80°$. Image acquisition was conducted for 30 s. In Study 2, three contiguous axial imaging planes containing auditory cortex were collected. TR = 0.5 s. $\theta = 60°$. Image acquisition was conducted for 20 s.

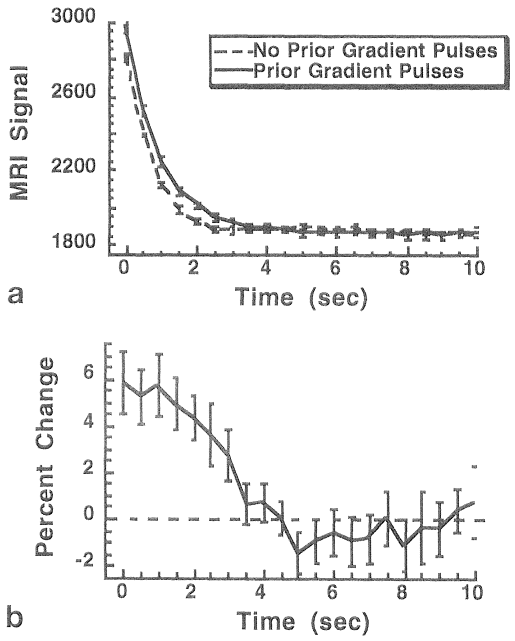

FIG. 7. (a) Average MRI signal from the five "control" and "task" trials in Fig. 6. (b) Average fractional difference signal between the "control" and "task" trials. Again, the difference returns to zero at about 5 s.

In Study 3, one axial plane containing motor cortex was obtained. TR = 0.5 s, $\theta = 60°$. For the "task" time series, bilateral self paced finger tapping was performed for 20 s prior to and through the 30 s of image acquisition. For the "control" time series, bilateral self paced finger tapping was begun at the start of image acquisition and continued throughout the time series. As a comparison and a verification of motor cortex regions, a time series was collected (TR = 1 s, repetitions = 130) of the same plane during finger movement for three 20 s on/off cycles. Correlation analysis with a box car reference function resembling a simplified expected response was performed to produce a functional image for comparison with the functional image produced by the technique used in Studies 1 and 2.

RESULTS

Study 1

Figures 2a and b show the first seven "task" and "control" images respectively, averaged from four trials each. The longitudinal magnetization reached steady state during this 7-s initial period. The images in Fig. 2c were produced by subtraction, at each time point, of the images in Fig. 2b from those in Fig. 2a. In these difference images, signal enhancement is clearly evident in the left and right auditory cortex until about five seconds, at which time the BOLD signal from the auditory cortex in Fig. 2b has had time to plateau in the "on" state. Since, at 7 s, both series are plateaued in the "on" state, a signal difference is no longer present.

Figure 3 shows the MR signal, during each of the four interleaved "task" trials indicated by "T," and "control" trials, indicated by "C," from 12 voxels in the auditory cortex. The peaks indicate the first image in each trial (TR = ∞). In spite of trial to trial variability, the "task" trial showed consistently enhanced signal.

Figure 4a shows the averaged MR signal across the four "task" and "control" trials Fig. 3. The BOLD signal in the auditory cortex was significantly enhanced for the "task" relative to the "control" series during the approach to steady state longitudinal magnetization. The percent change signal is shown in Fig. 4b.

For correlation analysis, the signal from an auditory cortex ROI of the "difference" time series, shown in Fig. 4c, was used as a reference function. Only the first seven time points were used in the calculation. The correlation coefficient of this unsmoothed difference signal with the "difference" time series was calculated on a voxel-wise basis. The anatomical echo planar images and corresponding functional images are shown in Figs. 5a and 5b, respectively. Enhancement in the primary auditory cortex is clearly shown.

For comparison, correlation analysis was performed on the same data set using a synthesized reference function shown in Fig. 4d. This function was created by first convolving an impulse response function, having properties derived from experimental studies using brief stimulus durations (16, 17), with a step function, then subtracting of this waveform from a simple "on" state function. The correlation images are shown in Fig. 5c. These images appear similar to those in Fig. 5b.

Study 2

The primary difference between Study 2 and Study 1 is that a TR of 500 ms was used instead of a TR of 1000 ms. Also, five rather than four interleaved "task" and "control" trials were performed.

Figure 6 shows the MRI signal, during each of the five interleaved "task" and "control" trials, from auditory cortex. Again, the peaks indicate the first image in each trial.

Figures 7a shows the averaged signal, across the five "task" and "control" trials in Fig. 6. The BOLD signal in the auditory cortex during the "task" trial again shows significant enhancement relative to the "control" trial

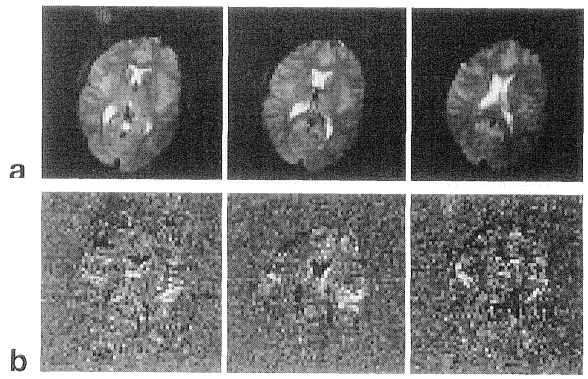

FIG. 8. (a) Anatomical images of the three slices obtained. (b) Functional images corresponding to the anatomical images. These were created in a similar manner as those in Fig. 5b.

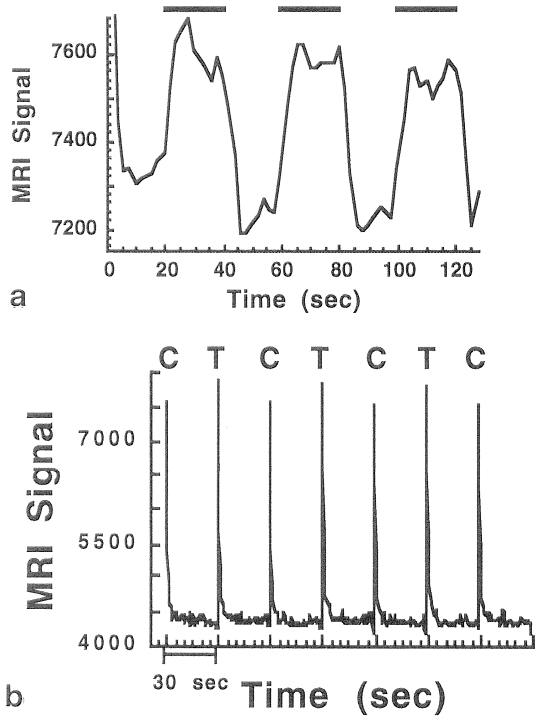

FIG. 9. (a) MRI signal from the motor cortex during cyclic 20 s off—20 s on finger movement. This signal was obtained from the identical motor cortex region as used in Fig. 10. (b) MRI signal from the identical motor cortex region as in Fig. 9a. In the task series, labeled "T," bilateral finger movement was performed for 20 s prior to image acquisition and throughout image acquisition without pause. In the control series labeled "C," finger movement was started simultaneously with the onset of time series image acquisition. The finger movement was performed to mimic auditory cortex activation demonstrated in the prior two studies.

during the approach to steady-state longitudinal magnetization. The percent change is shown in Fig. 7b. The onset time and latency of the BOLD signal increase is similar to that shown in Fig. 4b.

Anatomical and corresponding functional images are shown in Fig. 8 for the three imaging planes obtained. The functional images were created in a similar manner as in Study 1. Enhancement in the primary auditory cortex was similar.

Study 3

To further validate the technique, motor cortex activation maps were produced using a) conventional three-cycle 20 s off—20 s on paradigm in a single time series, and b) the technique described in Studies 1 and 2 during which motor cortex activation (sequential tapping of thumb to each of the other four fingers at a constant 4-finger opposition cycle rate of 2 Hz) was performed to mimic activation of the auditory cortex by imaging gradients for both "task" and "control" time series.

Figure 9a shows the MRI signal from the motor cortex during the cyclic 20 s off—20 s on time series. Figure 9b shows the MRI signal from the identical region of interest during interleaved "control" and "task" series. Figure 10a shows the averaged MRI signal from Fig. 9b. The fractional signal difference signal, shown in Figure 10b, demonstrates the same shape and latency as in Figs. 4b and 7b.

Functional images were created from the two techniques. First, the anatomical image of the slice chosen for analysis is shown in Fig. 11a. For the cyclic off-on series, correlation coefficient calculation of a box car reference function resembling the expected response with every voxel in the time series of images was used to create the functional image in Fig. 11b. The functional image in Fig. 11c was created by correlation coefficient calculation of the averaged difference signal from the motor cortex (used as a reference function) with the time series of difference images. The functional image in Fig. 11b has higher contrast to noise and reduced artifact than the functional image in Fig. 11c, but the locations of activation are nearly identical. These results suggest that this method, while not optimal for studies that can be performed in a more conventional manner, is a valid way to map cortical activation by the noise produced by MRI gradient switching.

DISCUSSION AND CONCLUSIONS

Human brain activation produced by the noise of EPI gradients has been mapped using a technique that incorporates subtraction of the first several seconds of a time series in which no prior EPI gradients were applied from the first several seconds of a time series in which EPI

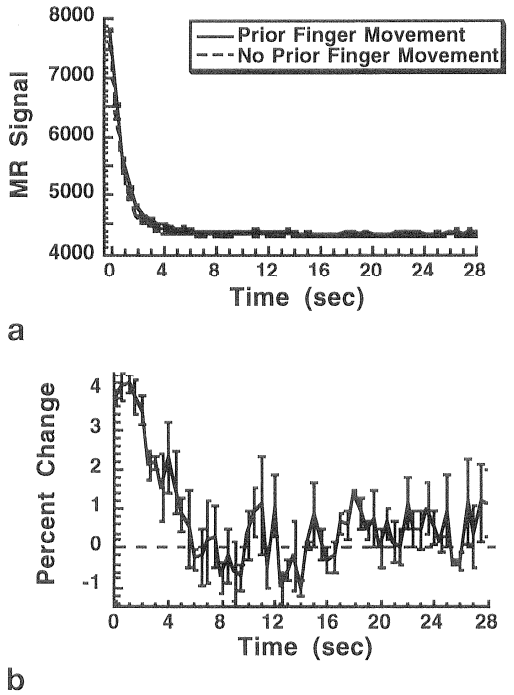

FIG. 10. (a) Average fractional difference signal between the "control" and "task" motor cortex trials. Again, the difference returns to zero at about 5 s. (b) Average fractional difference signal between the "control" and "task" series. Again, the difference returns to zero at about 5 s. This response is nearly identical to those shown in Fig. 4b and Fig. 7b.

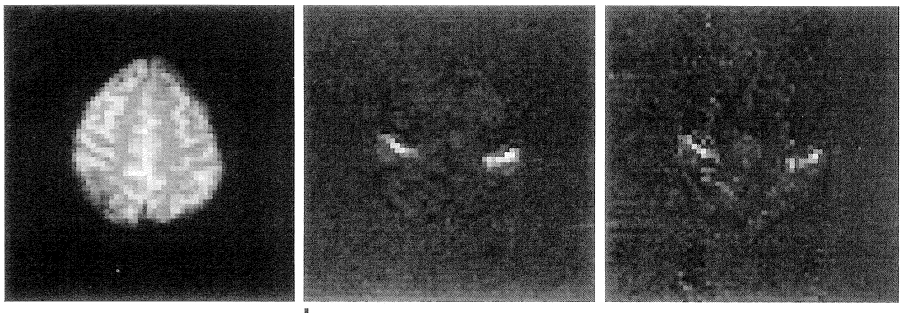

FIG. 11. (a) Anatomical image containing motor cortex. (b) Functional correlation image of motor cortex activation created using the more conventional cyclic activation paradigm in conjunction with correlation analysis. The time series plot from the motor cortex corresponding to this functional image is shown in Fig. 9. A boxcar function was used as the reference waveform. (c) Functional image created by the method for observing auditory cortex activation by the imaging gradient acoustic noise presented in Studies 1 and 2. The functional image was created by calculation of the correlation coefficient of the difference signal from the motor cortex with the difference time series. The time two time series plots corresponding to this functional image are shown in Fig. 10. Although the functional contrast to noise is less in Fig. 11c, the regions of activation are nearly identical.

gradients were applied for 20 s prior to time series collection.

The technique was demonstrated with a TR of 1000 and 500 ms. Furthermore, the technique was validated by comparison with a well characterized motor cortex activation paradigm.

For all subjects, activation by the acoustic noise of the EPI gradient pulses was observed in the auditory cortex. Because the TR and number of slices imaged were varied across subjects, the EPI pulse frequency varied. This variation did appear not cause significant differences in the location or degree of activation.

An experimental issue is that, to allow for the BOLD contrast change to fully plateau, the "task" stimuli was present for about 20 s prior to the start of image collection. If neuronal activation habituated during the 20 s of stimulation or showed an initial burst of activity only during the first 7 s, then, after subtraction, negative signal changes would be seen. The preliminary data indicate some negative changes. The data also suggest that subcortical activation may be present. Further study involving increased averaging, increased brain coverage, and modulated time duration of the preimaging gradient switching should clarify these activations.

The acoustic noise produced by EPI, while highly broadband in nature, appears to reside primarily in the gradient switching frequency of about 2 to 2.5 kHz (8). The acoustic noise of FLASH is different from EPI in that the peak amplitude is below 1 kHz, yet similar in that it is also somewhat broadband (18). It is difficult to predict how brain activation would vary across these scanning techniques.

Preliminary data from a method which involved having the subject listen to taped scanner noise at a higher volume than the scanner has been presented (19). While the results of this technique appear similar to those presented in this paper, the two techniques differ. The technique demonstrated here observed scanner noise-induced activation relative to a baseline of virtual silence. The technique of Ulmer *et al.* (19) involved a baseline in which activation by scanner noise was already present. The similarity of this approach to the one presented in the paper depends on whether or not: a) the hemodynamic response is saturated in the "on" state and b) all auditory activation is amplitude modulated.

A more general and still open question is whether or not neuronal and/or hemodynamic saturation occurs in any cortical region by the scanner noise. A careful comparison of the two techniques (relative locations and magnitudes of activation) is one means by which these questions can be tested. The technique presented in this paper supplies a method by which this comparison can be performed. Virtually any auditory stimuli could be presented in the identical manner as the gradient switching noise was presented in the paper. The magnitudes and areas of activation could be compared with those elicited by the same stimuli presented in an on/off manner during time series collection. Any differences in activation would be due to the masking effect of the scanner noise.

Future efforts in tonotopic mapping may benefit from paradigms designed to take MRI gradient acoustic noise induced activation into account. One can imagine tonotopic mapping paradigms that involve a "control" series of tone presentation once scanning has begun, and, a "task" series of tone presentation given prior to image acquisition and continued on through image acquisition. Subtraction of the first 5 s of these time series should reveal more clearly tonotopic maps that are uncorrupted by activation from noise produced by the scanner. Tonotopic mapping studies, using this technique, are currently being performed in this laboratory.

ACKNOWLEDGMENTS

The authors thank Shirley Eskridge for expert technical assistance and Jeffrey Binder, MD, for useful discussions.

REFERENCES

1. S. Ogawa, D. W. Tank, R. Menon, J. M. Ellermann, S.-G. Kim, H. Merkle, K. Ugurbil, Intrinsic signal changes accompanying sensory stimulation: functional brain mapping with magnetic resonance imaging. *Proc. Natl. Acad. Sci. USA* **89,** 5951–5955 (1992).
2. P. A. Bandettini, E. C. Wong, R. S. Hinks, R. S. Tikofsky, J. S. Hyde, Time course EPI of human brain function during task activation. *Magn. Reson. Med.* **25,** 390–397 (1992).
3. K. K. Kwong, J. W. Belliveau, D. A. Chesler, I. E. Goldberg, R. M. Weisskoff, B. P. Poncelet, D. N. Kennedy, B. E. Hoppel, M. S. Cohen, R. Turner, H. M. Cheng, T. J. Brady, B. R. Rosen, Dynamic magnetic resonance imaging of human brain activity during primary sensory stimulation. *Proc. Natl. Acad. Sci. USA* **89,** 5675–5679 (1992).

4. J. Frahm, H. Bruhn, K.-D. Merboldt, W. Hanicke, D. Math, Dynamic MR imaging of human brain oxygenation during rest and photic stimulation. *J. Magn. Reson. Imaging* **2,** 501–505 (1992).
5. J. R. Binder, S. M. Rao, T. A. Hammeke, F. Z. Yetkin, A. Jesmanowicz, P. A. Bandettini, E. C. Wong, L. D. Estkowski, M. D. Goldstein, V. M. Haughton, J. S. Hyde, Functional magnetic resonance imaging of human auditory cortex. *Ann. Neurol.* **35,** 662–672 (1994).
6. T. M. Talavage, P. J. Ledden, M. I. Sereno, R. R. Benson, B. R. Rosen, Preliminary fMRI evidence for tonotopicity in human auditory cortex. *NeuroImage* **3,** S355 (1996).
7. C. L. Kussmaul, C. M. Wessinger, M. H. Buonocore, G. R. Mangun, Tonotopic organization of human auditory cortex demonstrated with BOLD functional magnetic resonance imaging, *in* "Proc., Society for Neuroscience, 26th Annual Meeting, 1996," p. 1070.
8. C. M. Wessinger, M. H. Buonocore, C. L. Kussmaul, G. R. Mangun, Tonotopy in human auditory cortex examined with functional magnetic resonance imaging. *Hum. Brain Map.* **5,** 18–25 (1997).
9. E. A. DeYoe, P. Bandettini, J. Neitz, D. Miller, P. Winans, Functional magnetic resonance imaging (FMRI) of the human brain. *J. Neurosci. Methods* **54,** 171–187 (1994).
10. K. J. Friston, P. Jezzard, R. Turner, Analysis of functional MRI time-series. *Hum. Brain Map.* **1,** 153–171 (1994).
11. G. M. Boynton, S. A. Engel, G. H. Glover, D. J. Heeger, Linear systems analysis of functional magnetic resonance imaging in human V1. *J. Neurosci.* **16,** 4207–4221 (1996).
12. S. Ogawa, T. M. Lee, A. R. Kay, D. W. Tank, Brain magnetic resonance imaging with contrast dependent on blood oxygenation. *Proc. Natl. Acad. Sci. USA* **87,** 9868–9872 (1990).
13. E. C. Wong, P. A. Bandettini, J. S. Hyde, Echo-planar imaging of the human brain using a three axis local gradient coil, *in* "Proc., SMRM, 11th Annual Meeting, Berlin, 1992," p. 105.
14. E. C. Wong, G. Tan, J. S. Hyde, A quadrature transmit-receive end-capped birdcage coil for imaging of the human head at 125 MHz, *in* "Proc., SMRM, 12th Annual Meeting, New York, 1993," p. 1344.
15. P. A. Bandettini, A. Jesmanowicz, E. C. Wong, J. S. Hyde, Processing strategies for time-course data sets in functional MRI of the human brain. *Magn. Reson. Med.* **30,** 161–173 (1993).
16. P. A. Bandettini, E. C. Wong, E. A. DeYoe, J. R. Binder, S. M. Rao, D. Birzer, L. D. Estkowski, A. Jesmaniowicz, R. S. Hinks, J. S. Hyde, The functional dynamics of blood oxygen level dependent contrast in the motor cortex, *in* "Proc., SMRM, 12th Annual Meeting, New York, 1993," p. 1382.
17. P. A. Bandettini, E. C. Wong, J. R. Binder, S. M. Rao, A. Jesmanowicz, E. A. Aaron, T. F. Lowry, H. V. Forster, R. S. Hinks, J. S. Hyde, *in* "Diffusion and Perfusion: Magnetic Resonance Imaging" (D. LeBihan, Ed.), pp. 335–349, Raven Press, New York, 1995.
18. S. A. Counter, A. Olofsson, H. F. Grahn, E. Borg, MRI acoustic noise: sound pressure and frequency analysis. *J. Magn. Reson. Imaging* **7,** 606–611 (1997).
19. J. L. Ulmer, L. D. Estkowski, F. Z. Yetkin, J. C. Strainer, Functional MR imaging of the auditory cortex: cortical activation response to ambient scanner noise, *in* "Proc., Radiologic Society of North America, 82nd Annual Meeting, Chicago, 1996," p. 373.